

Synthesis, Structures, and Spectroscopy of the Metallostannylenes $(\eta^5\text{-C}_5\text{H}_5)(\text{CO})_3\text{M}-\text{Sn}-\text{C}_6\text{H}_3\text{-2,6-Ar}_2$ ($\text{M} = \text{Cr, Mo, W}$; $\text{Ar} = \text{C}_6\text{H}_2\text{-2,4,6-Me}_3, \text{C}_6\text{H}_2\text{-2,4,6-Pr}^i_3$)

Barrett E. Eichler, Andrew D. Phillips, Scott T. Haubrich,
Benjamin V. Mork, and Philip P. Power*

Department of Chemistry, University of California, Davis, One Shields Avenue,
Davis, California 95616

Received July 22, 2002

The metallostannylene compounds $(\eta^5\text{-C}_5\text{H}_5)(\text{CO})_3\text{MSn-C}_6\text{H}_3\text{-2,6-Me}_2$ ($\text{Mes} = \text{C}_6\text{H}_2\text{-2,4,6-Me}_3$; $\text{M} = \text{Cr}$ (**1**), Mo (**2**), W (**3**)), $(\eta^5\text{-C}_5\text{H}_5)(\text{CO})_3\text{MSn-C}_6\text{H}_3\text{-2,6-Trip}_2$ ($\text{Trip} = \text{C}_6\text{H}_2\text{-2,4,6-Pr}^i_3$; $\text{M} = \text{Cr}$ (**4**), Mo (**5**), W (**6**)), and $(\eta^5\text{-1,3-Bu}^t\text{C}_6\text{H}_3)\text{MoSn-C}_6\text{H}_2\text{-2,6-Trip}_2$ (**7**) were synthesized by the reaction of the appropriate aryltin(II) halide with the alkali-metal salt of the cyclopentadienylcarbonylmetalate. The compounds, which were isolated as purple (**1–6**) or turquoise (**7**) crystals, are monomeric with V-shaped two-coordinate geometries at tin. The tin–transition-metal bonds are slightly longer than the distances predicted from metallic and covalent radii or those observed in related tin(IV)–transition-metal species. The compounds were also characterized by IR and UV–vis spectroscopy as well as ^1H , ^{13}C , and ^{119}Sn NMR spectroscopy. The ^{119}Sn NMR spectra displayed singlet resonances whose chemical shifts were in the range 2116–2650 ppm. These shifts were consistent with the two-coordination at tin. With use of ^{119}Sn NMR and UV–visible spectroscopic data for **1–7**, together with data for other two-coordinate tin(II) species, it was shown that there is a rough correlation between the ^{119}Sn NMR chemical shift and the wavelength of the n–p transition. This correlation underlines the importance of the paramagnetic shielding term in determining ^{119}Sn chemical shifts.

Introduction

The synthesis and characterization of $\text{Sn}\{\text{N}(\text{SiMe}_3)_2\}_2$ in 1974 represented the first example³ of a divalent, molecular tin(II) species (i.e., a stannylene) that proved to have a two-coordinate monomeric structure in the vapor and solution phases as well as in the solid state.^{3–5} In the ensuing period, ca. 40 neutral, two-coordinate tin(II) species have been structurally characterized.⁶ Of these, eight are heteroleptic species in which the two-coordinate tin is substituted by two different groups. The compounds have a V-shaped geometry and exist in the singlet state in which the lone pair occupies an orbital that is mainly 5s in character, leaving an empty tin 5p orbital. Electronic transitions between the lone pair and p orbital (n–p transitions)

are possible, and such transitions are responsible for their colors, which can vary between yellow and violet. The color is dependent on the excitation energy for the singlet–triplet transition, which in turn is governed by the electronic and steric properties of the substituents at tin. The ground-state–excited-state energy difference may also have a large effect on the ^{119}Sn NMR chemical shift through changes in paramagnetic shielding contributions.^{7,8} In fact, two-coordinate tin(II) species display a very wide chemical shift range of ca. 3200 ppm, with shifts that cannot be accounted for in terms of the σ -inductive effects of the substituents.⁷ Oddly, no two-coordinate tin(II) species in which the tin is substituted by a transition metal are known. In fact, with the exception of 2,6-Trip₂H₃C₆(Me)₂SnSnC₆H₃-2,6-Trip₂⁹ no stable, two-coordinate metallostannylenes have been described, although several complexes are known in which a stannylene acts as a ligand to a transition-metal center.¹⁰ The synthesis, spectroscopy, and structures of a series of metallostannylenes are now described, and their properties are discussed with reference to currently available data for other two-coordinate tin(II) species.

(1) Harris, D. H.; Lappert, M. F. *Chem. Commun.* **1994**, 895.

(2) Schaeffer, C. D.; Zuckerman, J. J. *J. Am. Chem. Soc.* **1974**, *96*, 7160.

(3) The first structural authentication of a monomeric two-coordinate tin(II) species in the crystal phase involved the compound $\text{SnN}(\text{Bu}^t\text{SiMe}_2)_2$: Veith, M. Z. *Naturforsch.* **1978**, *33B*, 7.

(4) The vapor-phase electron diffraction structure and X-ray crystal structure of $\text{Sn}\{\text{N}(\text{SiMe}_3)_2\}_2$ were reported in: Lappert, M. F.; Power, P. P.; Slade, M. J.; Hedberg, L.; Hedberg, K.; Schomaker, K. *Chem. Commun.* **1979**, 369. Fjeldberg, T.; Hope, H.; Lappert, M. F.; Power, P. P.; Thorne, A. J. *Chem. Commun.* **1983**, 639.

(5) The weakly Sn–Sn bonded, dimeric alkyl $[\text{Sn}\{\text{CH}(\text{SiMe}_3)_2\}_2]_2$, which is isoelectronic with $\text{Sn}\{\text{N}(\text{SiMe}_3)_2\}_2$, is also monomeric in the vapor phase and in dilute hydrocarbon solution: Fjeldberg, T.; Haaland, A.; Lappert, M. F.; Schilling, B. E. R.; Thorne, A. J. *J. Chem. Soc., Dalton Trans.* **1986**, 1551.

(6) Cambridge Crystallographic Data Centre: CSD version 5.23 (April 2002).

(7) Wrackmeyer, B. *Annu. Rep. NMR Spectrosc.* **1999**, *38*, 203.

(8) Eichler, B. E.; Phillips, B. L.; Power, P. P.; Augustine, M. P. *Inorg. Chem.* **2000**, *39*, 5450.

(9) Eichler, B. E.; Power, P. P. *Inorg. Chem.* **2000**, *39*, 5444. However, metallostannylenes with chelating ligands are known: Benet, S.; Cardin, C. J.; Cardin, D. J.; Constantine, S. P.; Heath, P.; Rashid, H.; Teixeira, S.; Thorpe, J. H.; Todd, A. K. *Organometallics* **1999**, *18*, 389.

(10) Lappert, M. F.; Rowe, R. S. *Coord. Chem. Rev.* **1990**, *100*, 267.

Experimental Section

General Procedures. All manipulations were carried out by using modified Schlenk techniques under an atmosphere of N₂ or in a Vacuum Atmospheres HE-43E drybox. All solvents were freshly distilled from potassium and degassed three times before use. The compounds Sn(Cl)C₆H₃-2,6-Mes₂,¹¹ Sn(Cl)C₆H₃-2,6-Trip₂,¹² NaM(η⁵-C₅H₅)(CO)₃,^{13a} NaM(η⁵-C₅H₅)(CO)₃·2DME^{13b} (M = Cr, Mo, W; DME = 1,2-dimethoxyethane), and KMo(η⁵-1,3-Bu^t₂C₅H₃)(CO)₃¹⁴ were prepared according to literature procedures. ¹H and ¹³C NMR data were recorded on either a General Electric QE-300 or Bruker Inova 400 and referenced with the respect to C₆D₆. ¹¹⁹Sn NMR spectra were obtained with a Bruker Inova 400 referenced to Sn(CH₃)₄ with 5% C₆D₆. Infrared data were recorded on a Perkin PE-1430 instrument. UV-vis data were recorded on a Hitachi-1200 instrument. Compounds 1–7 afforded satisfactory C, H analyses.

(η⁵-C₅H₅)(CO)₃MSnC₆H₃-2,6-Mes₂ (M = Cr (1), Mo (2), W (3)). A solution of Sn(Cl)C₆H₃-2,6-Mes₂¹¹ (2 mmol) in (ca. 40 mL) toluene was added over a period of ca. 1 h to a rapidly stirred slurry of 2 mmol of Na(η⁵-C₅H₅)M(CO)₃ (M = Cr, Mo, W) in toluene (10 mL) with cooling to ca. -78 °C in a dry ice bath.⁹ The reaction mixture was warmed to room temperature overnight. Stirring was discontinued, the solids were allowed to settle, and the supernatant liquid was decanted. The solution was reduced in volume to incipient crystallization and stored in a ca. -20 °C freezer overnight, to afford crystals of the products (η⁵-C₅H₅)(CO)₃MSnC₆H₃-2,6-Mes₂. **1** (M = Cr): purple crystals, yield 0.43 g (0.68 mmol, 34%). Mp: 190–191 °C. ¹H NMR (399.77 MHz, C₆D₆, 25 °C): δ 2.05 (s, 6H, *p*-CH₃), 2.14 (s, 12H, *o*-CH₃), 3.70 (s, 5H, η⁵-C₅H₅), 6.74 (s, 4H, *m*-C₆H₃), 7.20 (d, ³J_{HH} = 7.50 Hz, 2H, *m*-C₆H₃), 7.43 (t, ³J_{HH} = 7.50 Hz, *p*-C₆H₃). ¹³C{¹H} NMR (100.53 MHz, C₆D₆, 25 °C): δ 21.51 (s, *p*-CH₃), 21.86 (s, *o*-CH₃), 88.87 (s, η⁵-C₅H₅), 129.60 (*o*-Mes), 130.01 (*o*-C₆H₃), 130.57 (s, *m*-Mes), 136.42 (s, *m*-C₆H₃), 136.71 (s, *p*-C₆H₃), 138.35 (s, *p*-Mes), 146.43 (s, *i*-Mes), 186.10 (s, *i*-C₆H₃), 235.25 (br. m, CO). ¹¹⁹Sn{¹H} NMR (149.25 MHz, C₆D₆, 25 °C): δ 2319 (s). IR (Nujol, cm⁻¹): 1960 s, 1905 s, 1878 s. UV-vis (hexane): λ_{max} 577 nm. Anal. Calcd for C₃₂H₃₀O₃-CrSn: C, 60.69; H, 4.78. Found: C, 60.73; H, 5.01. **2** (M = Mo): dark purple crystals, yield 0.69 g (1.01 mmol, 51%). Mp: 206–209 °C dec. ¹H NMR (399.77 MHz, C₆D₆, 25 °C): δ 2.07 (s, 6H, *p*-CH₃), 2.45 (s, 12H, *o*-CH₃), 4.25 (s, 5H, η⁵-C₅H₅), 6.73 (s, 4H, *m*-C₆H₃), 7.20 (d, ³J_{HH} = 7.50 Hz, 2H, *m*-C₆H₃), 7.43 (t, ³J_{HH} = 7.50 Hz, *p*-C₆H₃). ¹³C{¹H} NMR (100.53 MHz, C₆D₆, 25 °C): δ 20.89 (s, *p*-CH₃), 21.25 (s, *o*-CH₃), 92.28 (s, η⁵-C₅H₅), 129.14 (s, *o*-Mes), 129.42 (*o*-C₆H₃), 129.90 (*m*-Mes), 135.82 (s, *m*-C₆H₃), 135.59 (s, *p*-C₆H₃), 137.59 (s, *p*-Mes), 145.86 (s, *i*-Mes), 184.54 (s, *i*-C₆H₃), 226.63 (br. m, CO). ¹¹⁹Sn{¹H} NMR (149.25 MHz, C₆D₆, 25 °C): δ 2116 (s). IR (Nujol, cm⁻¹): 1960 s, 1915 s, 1975 s. UV-vis (hexane): λ_{max} 569 nm. Anal. Calcd for C₃₂H₃₀O₃MoSn: C, 56.75; H, 4.47. Found: C, 56.21; 4.28. **3** (M = W): dark purple crystals, yield 0.64 g (0.84 mmol, 42%). Mp: 202–204 °C dec. ¹H NMR (399.77 MHz, C₆D₆, 25 °C): δ 2.06 (s, 6H, *p*-CH₃), 2.45 (s, 12H, *o*-CH₃), 4.24 (s, 5H, η⁵-C₅H₅), 6.73 (s, 4H, *m*-C₆H₃), 7.20 (d, ³J_{HH} = 7.20 Hz, 2H, *m*-C₆H₃), 7.43 (t, ³J_{HH} = 7.20 Hz, *p*-C₆H₃). ¹³C{¹H} NMR (100.53 MHz, C₆D₆, 25 °C): δ 21.48 (s, *p*-CH₃), 21.90 (s, *o*-CH₃), 91.21 (s, η⁵-C₅H₅), 129.22 (s, *o*-Mes), 129.91 (*o*-C₆H₃), 130.76 (s, *m*-Mes), 136.44 (s, *m*-C₆H₃), 136.55 (s, *p*-C₆H₃), 138.06 (s, *p*-Mes), 146.37 (s, *i*-Mes), 182.97 (s, *i*-C₆H₃), 216.69 (br. m, CO). ¹¹⁹Sn{¹H} NMR (149.25 MHz, C₆D₆, 25 °C): δ 2367 (s). IR (Nujol, cm⁻¹):

1960 s, 1920 s, 1890 s. UV-vis (hexane): λ_{max} 559 nm. Anal. Calcd for C₃₂H₃₀O₃WSn: C, 50.23; H, 3.95. Found: C, 50.74; H, 3.71.

(η⁵-C₅H₅)(CO)₃MSnC₆H₃-2,6-Trip₂ (M = Cr (4), Mo (5), W (6)). A solution of Sn(Cl)C₆H₃-2,6-Trip₂⁹ (1 mmol) in toluene (ca. 20 mL) was added to a rapidly stirred solution of 1 mmol of Na[M(η⁵-C₅H₅)(CO)₃]·2DME¹⁰ (where M is Cr, Mo, or W) in toluene (ca. 15 mL) with cooling to ca. 0 °C. The solution was stirred for an additional 2 h and allowed to come to ambient temperature. All volatile materials were removed under reduced pressure, and the remaining solid was extracted with hexane (ca. 30 mL). The resulting solution was filtered through a Celite-padded frit and concentrated to incipient crystallization. The solution was stored at ca. -20 °C for several days to yield crystals of the product 2,6-Trip₂C₆H₃SnM(η⁵-C₅H₅)(CO)₃. **4** (M = Cr): purple crystals, yield 0.22 g, (0.28 mmol, 28%). Mp: 209–210 °C dec. ¹H NMR (300.65 MHz, C₆H₆, 25 °C): δ 1.12 (d, ³J_{HH} = 6.9 Hz, 24H, *o*-CH(CH₃)₂), 1.18 (d, ³J_{HH} = 6.9 Hz, 24H, *o*-CH(CH₃)₂), 1.45 (d, ³J_{HH} = 6.9 Hz, 12H, *p*-CH(CH₃)₂), 2.74 (sept, ³J_{HH} = 6.9 Hz, 2H, *p*-CH(CH₃)₂), 3.48 (br m, 4H, *o*-CH(CH₃)₂), 3.71 (s, 5H, η⁵-C₅H₅), 7.13 (br m, 3H, *p*- and *m*-C₆H₃), 7.43 (s, 4H, *m*-Trip). ¹³C{¹H} NMR (75.61 MHz, C₆D₆, 25 °C): δ 23.11 (s, *o*-CH(CH₃)₂), 24.09 (s, *o*-CH(CH₃)₂), 27.34 (s, *p*-CH(CH₃)₂), 31.07 (s, *o*-CH(CH₃)₂), 34.81 (s, *p*-CH(CH₃)₂), 88.28 (s, η⁵-C₅H₅), 122.08 (s, *m*-Trip), 128.28 (s, *p*-C₆H₃), 130.82 (s, *m*-C₆H₃), 133.81 (s, *i*-Trip), 144.93 (s, *p*-Trip), 147.66 (s, *o*-Trip), 149.71 (s, *o*-C₆H₃), 187.07 (s, *i*-C₆H₃), 233.90 (br. m, CO). ¹¹⁹Sn{¹H} NMR (149.25 MHz, C₆H₆, 25 °C): δ 2298 (s). IR (Nujol, cm⁻¹): 1963 s, 1892 s, 1868 s. UV-vis (hexane): λ_{max} 574 nm. Anal. Calcd for C₄₄H₅₄O₃CrSn: C, 65.93; H, 6.79. Found: C, 66.28; H, 6.77. **5** (M = Mo): dark purple crystals, yield 0.52 g (0.62 mmol, 61%). Mp: 161 °C dec. ¹H NMR (300.65 MHz, C₆H₆, 25 °C): δ 1.19 (d, ³J_{HH} = 6.9 Hz, 24H, *o*-CH(CH₃)₂), 1.45 (d, ³J_{HH} = 6.9 Hz, 12H, *p*-CH(CH₃)₂), 2.75 (sept, ³J_{HH} = 6.9 Hz, 2H, *p*-CH(CH₃)₂), 3.46 (br m, 2H, *o*-CH(CH₃)₂), 3.61 (br m, 2H, *o*-CH(CH₃)₂), 4.25 (s, 5H, η⁵-C₅H₅), 7.06 (br m, 1H, *p*-C₆H₃), 7.21 (br m, 2H, *m*-C₆H₃), 7.42 (s, 4H, *m*-Trip). ¹³C{¹H} NMR (75.61 MHz, C₆D₆, 25 °C): δ 22.99 (s, *o*-CH(CH₃)₂), 23.50 (s, *o*-CH(CH₃)₂), 24.13 (s, *o*-CH(CH₃)₂), 26.68 (s, *o*-CH(CH₃)₂), 27.87 (s, *p*-CH(CH₃)₂), 30.59 (s, *o*-CH(CH₃)₂), 31.46 (s, *p*-CH(CH₃)₂), 34.77 (s, *o*-CH(CH₃)₂), 92.52 (s, η⁵-C₅H₅), 121.39 (s, *m*-Trip), 122.82 (s, *m*-Trip), 127.66 (s, *p*-C₆H₃), 130.68 (s, *m*-C₆H₃), 133.49 (s, *i*-Trip), 144.92 (s, *p*-Trip), 146.21 (s, *o*-Trip), 148.73 (s, *o*-Trip), 149.52 (s, *o*-C₆H₃), 185.01 (s, *i*-C₆H₃), 224.79 (br m, CO), 228.51 (br m, CO). ¹¹⁹Sn{¹H} NMR (149.25 MHz, C₆H₆, 25 °C): δ 2414 (s). IR (Nujol, cm⁻¹): 2020 s, 1952 s, 1922 s. UV-vis (hexane): λ_{max} 575 nm. Anal. Calcd for C₄₄H₅₄O₃MoSn: C, 62.50; H, 6.44. Found: C, 62.95; H, 6.31. **6** (M = W): dark purple crystals, yield 0.35 g, (0.34 mmol, 34%). Mp: 196–198 °C dec. ¹H NMR (300.65 MHz, C₆H₆, 25 °C): δ 1.20 (d, ³J_{HH} = 6.9 Hz, 24H, *o*-CH(CH₃)₂), 1.46 (d, ³J_{HH} = 6.9 Hz, 12H, *p*-CH(CH₃)₂), 2.76 (sept, ³J_{HH} = 6.9 Hz, 2H, *p*-CH(CH₃)₂), 3.55 (br m, 4H, *o*-CH(CH₃)₂), 4.25 (s, 5H, η⁵-C₅H₅), 7.07 (t, ³J_{HH} = 7.50 Hz, 1H, *p*-C₆H₃), 7.20 (d, ³J_{HH} = 7.50 Hz, 2H, *m*-C₆H₃), 7.41 (s, 4H, *m*-Trip). ¹³C{¹H} NMR (75.46 MHz, C₆D₆, 25 °C) δ 23.83 (s, *o*-CH(CH₃)₂), 24.30 (s, *o*-CH(CH₃)₂), 25.23 (s, *o*-CH(CH₃)₂), 27.15 (s, *p*-CH(CH₃)₂), 31.59 (s, *o*-CH(CH₃)₂), 31.48 (s, *o*-CH(CH₃)₂), 34.79 (s, *p*-CH(CH₃)₂), 91.59 (s, η⁵-C₅H₅), 121.39 (s, *m*-Trip), 122.74 (s, *m*-Trip), 129.13 (s, *p*-C₆H₃), 131.23 (s, *m*-C₆H₃), 144.91 (s, *i*-Trip), 147.09 (s, *p*-C₆H₃), 148.08 (s, *o*-Trip), 148.71 (s, *o*-Trip), 149.39 (s, *o*-C₆H₃), 183.07 (s, *i*-C₆H₃) 215.05 (br m, CO). ¹¹⁹Sn{¹H} NMR (149.46 MHz, C₆H₆, 25 °C): δ 2650 (s). IR (Nujol, cm⁻¹): 1962 s, 1891 s, 1870 s. UV-vis (hexane): λ_{max} 570 nm. Anal. Calcd for C₄₄H₅₄O₃WSn: C, 56.61; H, 5.83. Found: C, 57.04; H, 5.82.

(η⁵-1,3-Bu^t₂C₅H₃)(CO)₃MoSnC₆H₃-2,6-Trip₂ (7) was prepared using a method analogous to the synthesis of **5**. Compound **7** was obtained as turquoise crystals: yield 0.41 g (0.43 mmol, 43%). Mp: 188–189 °C dec. ¹H NMR (300.77 MHz, C₆H₆, 25 °C): δ 1.09 (s, 18H, η⁵-((CH₃)₃C)₂C₅H₃), 1.22 (d, ³J_{HH}

(11) Simons, R.; Pu, L.; Olmstead, M. M.; Power, P. P. *Organometallics* **1997**, *16*, 1920–1925.

(12) Pu, L.; Senge, M. O.; Olmstead, M. M.; Power, P. P. *J. Am. Chem. Soc.* **1998**, *120*, 12682.

(13) (a) Behrens, U.; Edelmann, F. *J. Organomet. Chem.* **1984**, *263*, 179–182. (b) Braunstein, P. *Inorg. Synth.* **1989**, *26*, 343.

(14) Scheer, M.; Friedrich, G.; Kay, S. *Angew. Chem., Int. Ed. Engl.* **1993**, *32*, 593–594.

Table 1. Crystallographic Data for Compounds 1–7

	1	2	3	4	5	6	7
formula	C ₃₂ H ₃₀ O ₃ CrSn	C ₃₂ H ₃₀ O ₃ MoSn	C ₃₂ H ₃₀ O ₃ WSn	C ₄₄ H ₅₄ O ₃ CrSn	C ₄₄ H ₅₄ O ₃ MoSn	C ₄₄ H ₅₄ O ₃ WSn	C ₅₂ H ₇₀ O ₃ MoSn
fw	633.25	677.19	765.10	801.56	845.50	933.41	957.71
color, habit	purple, parallelepiped	dark red, parallelepiped	red, parallelepiped	purple, needle	purple, prism	red-purple, prism	green-blue, cube
cryst syst	triclinic	triclinic	triclinic	monoclinic	monoclinic	monoclinic	monoclinic
space group	<i>P</i> 1	<i>P</i> 1	<i>P</i> 1	<i>P</i> 2 ₁ / <i>c</i>	<i>P</i> 2 ₁ / <i>c</i>	<i>P</i> 2 ₁ / <i>c</i>	<i>C</i> 2/ <i>c</i>
<i>a</i> , Å	8.4349(15)	8.474(2)	8.446(2)	19.575(2)	19.710(5)	19.6411(7)	42.799(1)
<i>b</i> , Å	9.9869(15)	10.047(2)	10.017(3)	10.526(1)	10.590(2)	10.5712(4)	13.4191(4)
<i>c</i> , Å	17.211(2)	17.273(4)	17.240(4)	19.613(2)	19.359(6)	19.3085(7)	17.8045(6)
α, deg	85.493(12)	85.43(3)	85.29(2)				
β, deg	78.463(13)	79.42(3)	79.52(2)	91.363(2)	90.45(2)	90.392(1)	107.997(1)
γ, deg	75.818(12)	75.56(3)	75.53(2)				
<i>Z</i>	2	2	2	4	4	4	4
<i>V</i> , Å ³	1376.5(4)	1399.0(5)	1387.7(6)	4039.7(8)	4040.7(18)	4008.9(3)	9725.3(5)
ρ, g cm ⁻³	1.528	1.608	1.831	1.318	1.390	1.566	1.308
cryst dims, mm	0.15 × 0.08 × 0.03	0.50 × 0.50 × 0.40	0.32 × 0.06 × 0.04	0.39 × 0.25 × 0.17	0.50 × 0.36 × 0.24	0.22 × 0.10 × 0.10	0.10 × 0.10 × 0.09
2θ range, deg	2.62–56.40	2.09–27.56	2.61–56.34	2.08–60.00	4.14–55.00	2.08–46.00	3.80–63.08
μ, mm ⁻¹	10.709	1.372	14.947	0.924	0.965	3.528	0.810
no. of unique data	3594	6443	3644	11 743	10 076	57 980	71 229
no. of data with <i>I</i> > 2σ(<i>I</i>)	2794	5383	3319	6777	9280	5244	15 688
no. of params	340	335	340	442	462	451	724
R1 (<i>I</i> > 2σ(<i>I</i>))	0.060	0.0397	0.0524	0.0504	0.0458	0.0393	0.0423
wR2 (all data)	0.015	0.1054	0.1473	0.1181	0.1070	0.1644	0.1068

= 6.9 Hz, 12H, *p*-CH(CH₃)₂), 1.50 (br d, ³J_{HH} = 6.9 Hz, 24H, *o*-CH(CH₃)₂), 2.78 (sept, ³J_{HH} = 6.9 Hz, 2H, *p*-CH(CH₃)₂), 3.51 (br s, 4H, *o*-CH(CH₃)₂), 3.82 (d, ⁴J_{HH} = 1.90 Hz, 2H, η⁵-((CH₃)₃C)₂C₅H₃), 5.31 (t, ⁴J_{HH} = 1.90 Hz, 1H, η⁵-((CH₃)₃C)₂C₅H₃), 7.16 (t, ³J_{HH} = 7.50 Hz, 1H, *p*-C₆H₃), 7.45 (d, ³J_{HH} = 7.50 Hz, 2H, *m*-C₆H₃), 7.45 (s, 4H, *m*-Trip). ¹³C{¹H} NMR (100.53 MHz, C₆D₆, 25 °C): δ 23.31 (br s, *o*-CH(CH₃)₂), 24.14 (s, *p*-CH(CH₃)₂), 31.13 (br s, *o*-CH(CH₃)₂), 31.89 (s, *p*-CH(CH₃)₂), 32.39 (s, η⁵-((CH₃)₃C)₂C₅H₃), 34.74 (s, η⁵-((CH₃)₃C)₂C₅H₃), 83.51 (s, η⁵-((CH₃)₃C)₂C₅H₃), 92.40 (η⁵-((CH₃)₃C)₂C₅H₃), 122.00 (br s, *m*-Trip), 127.02 (s, *p*-C₆H₃), 127.51 (s, η⁵-((CH₃)₃C)₂C₅H₃), 130.79 (s, *m*-C₆H₃), 133.93 (s, *i*-Trip), 145.20 (s, *p*-Trip), 147.09 (s, *o*-Trip), 149.33 (s, *o*-Trip), 185.89 (*i*-C₆H₃), 226.17 (br m, CO), 230.00 (br m, CO). ¹¹⁹Sn{¹H} NMR (149.46 MHz, C₆H₆, 25 °C): δ 2543 (s). IR (Nujol, cm⁻¹): 1959 s, 1888 s, 1858 s. UV-vis (hexane): λ_{max} 599 nm. Anal. Calcd for C₅₂H₇₀O₃MoSn: C, 65.21; H, 7.37. Found: C, 65.01; H, 7.03.

X-ray Data Collection, Solution, and Refinement. Crystals of a suitable quality for X-ray diffraction were coated rapidly with hydrocarbon oil, attached to a glass fiber, and frozen in place under a cold stream of N₂ on the diffractometer.¹⁵ Data for structures of **1** and **3** were obtained using a Siemens P4RA rotating anode diffractometer operating at 130 K using a Cu Kα radiation source (λ = 1.541 78 Å). The structures of **2** and **5** were obtained using a Siemens R3 diffractometer, at a temperature of 140 K using a Mo Kα radiation source (λ = 0.710 73 Å). The remaining structures were measured on a Bruker AXS SMART 1000 CCD diffractometer at 93 K using Mo Kα radiation (λ = 0.710 73 Å). Structural determination (solved by direct methods) and refinement (full-matrix least squares on *F*²) were performed using the SHELXTL¹⁶ suite of programs. Absorption corrections were applied to the structures of **1–3** and **5** using the program XABS2,¹⁷ and for the structures of **4**, **6**, and **7**, empirical corrections were added using SADABS.¹⁸ Hydrogen atoms were placed at calculated positions using a riding model

(15) Hope, H. *Prog. Inorg. Chem.* **1995**, *41*, 1.

(16) Sheldrick, G. M. SHELXL v5.10: Program Package for Refinement of Crystal Structures; University of Göttingen, Göttingen, Germany, 1989.

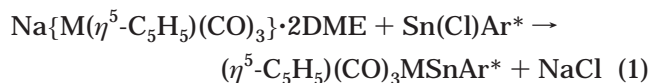
(17) Parkin, S.; Moezzi, B.; Hope, H. XABS2: An Empirical Absorption Correction Program. *J. Appl. Crystallogr.* **1995**, *28*, 53.

(18) SADABS is an empirical absorption correction program using the method described by: Blessing, R. H. *Acta Crystallogr.* **1995**, *A51*, 33. Sheldrick, G. M. SADABS; University of Göttingen, Göttingen, Germany, 1989.

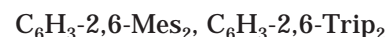
and were included in the refinement of the structure. All non-hydrogen atoms were anisotropically refined. The structures of **5** and **6** displayed a single disordered isopropyl group and were modeled using partial occupancies for the atoms involved. Specific details concerning data collection, solution, and refinement are given in Table 1.

Results and Discussion

Synthesis and Spectroscopy. The compounds **1–7** were synthesized in a straightforward manner by the reaction of 1 equiv of Sn(Cl)C₆H₃-2,6-Mes₂ or Sn(Cl)-C₆H₃-2,6-Trip₂ with Na{M(η⁵-C₅H₅)(CO)₃}·2DME (M = Cr, Mo, W) or K(η⁵-C₅H₅-1,3-Bu^t₂)·Mo(CO)₃ in toluene, as shown in eq 1. The compounds **1–6** were isolated in



M = Cr, Mo, W; Ar* =



moderate yields as dark purple crystals, whereas **7** was obtained as turquoise crystals. The bulkier cyclopentadienyl ligand η⁵-1,3-Bu^t₂-C₅H₃ was employed in complex **7** with the object of generating sufficient steric crowding to induce CO elimination and generate the multiply bonded species (η⁵-1,3-Bu^t₂-C₅H₃)(CO)₂MoSnC₆H₃-2,6-Trip₂ in a manner similar to that for their germanium analogues.¹⁹ However, this type of elimination was not observed under ambient conditions. The compounds were characterized by ¹H, ¹³C, and ¹¹⁹Sn NMR spectroscopy and by UV-vis and IR spectroscopy. The ¹H NMR spectra displayed absorptions due to the cyclopentadienyl and terphenyl ligands in a 1:1 intensity ratio. ¹³C NMR spectroscopy permitted identification of the 10 different terphenyl carbons in the cases of **1–3** plus absorptions due to the cyclopentadienyl and carbonyl carbons. Similar assignments could be made for the ¹³C NMR spectra of **4–7**, which exhibited two

(19) Pu, L.; Twamley, B.; Haubrich, S. T.; Olmstead, M. M.; Mork, B. V.; Simons, R. S.; Power, P. P. *J. Am. Chem. Soc.* **2000**, *122*, 650.

absorptions for the methyl groups of the *o*-Prⁱ substituents owing to their diastereotopic nature. The η^5 -C₅H₅ signals of the chromium complexes **1** and **4** (ca. 3.70 ppm) appear ca. 0.5 ppm upfield of the molybdenum and tungsten complexes **2**, **3**, and **5–7**. This pattern resembles that observed for the complexes $(\eta^5\text{-C}_5\text{H}_5)(\text{CO})_3\text{MSnMe}_3$ (M = Cr, Mo, W)²⁰ and is consistent with greater metal–ligand interactions for the molybdenum and tungsten complexes. The ¹H NMR η^5 -C₅H₅ signals in **1–6** are ca. 1 ppm upfield of those of the corresponding $(\eta^5\text{-C}_5\text{H}_5)(\text{CO})_3\text{MSnMe}_3$ (M = Cr, Mo, W) complexes, suggesting that the –SnAr ligands are more electron donating than –SnMe₃. The IR spectra of **1–7** each feature three absorptions in the carbonyl stretching region. Similar patterns have been previously reported in the corresponding germanium and lead derivatives. On average these are lower by 10–20 cm^{–1} than those observed for the $(\eta^5\text{-C}_5\text{H}_5)(\text{CO})_3\text{MSnMe}_3$ (M = Cr, Mo, W). This suggests greater electron density at the transition metals in **1–7**, which could result in greater back-bonding into the π^* orbitals of the carbonyls and, hence, lower CO stretching frequencies. These conclusions are in line with the ¹H NMR shifts for the η^5 -C₅H₅ resonances discussed above.

The electronic spectra of **1–7** are characterized by a single, moderately strong absorption which was observed in the wavelength range 559–577 nm. Intense absorptions below 300 nm were also observed. The longer wavelength absorptions are very probably due to an electronic transition from the tin lone pair to the p orbital. These absorptions fall within the range 476–689 nm^{21,22} previously observed for two-coordinate tin(II) organometallic species, and between the corresponding absorptions for germanium (396–420 nm)¹⁹ and lead analogues (611–616 nm)²³ of **1–7**. Furthermore, it can be noted that the related tin(IV) complexes $(\eta^5\text{-C}_5\text{H}_5)(\text{CO})_3\text{MSnMe}_3$ (M = Cr, Mo, or W), in which there is no possibility of n–p transitions involving the tin center, do not show absorptions near these wavelengths. Instead, their electronic spectra are characterized by intense absorptions below 300 nm which tail into the visible region and impart the characteristic yellow to orange-red colors of these species.

The compounds **1–7** were also characterized by ¹¹⁹Sn NMR spectroscopy. Their spectra display strong downfield shifts in the region 2116–2650 ppm. The chemical shifts of a range of monomeric, two-coordinate tin(II) species together with those of **1–7** are provided in Table 2 for comparison. Although a greater range of shifts is known,⁷ only species for which UV–vis data are also available are listed.^{22,24–32} It can be seen that the ¹¹⁹Sn

Table 2. ¹¹⁹Sn NMR Chemical Shifts and UV–Vis Data for Divalent Two-Coordinate Molecular Tin Compounds

	δ (¹¹⁹ Sn NMR)	λ_{max} (nm)	ref
Sn(C ₆ H ₃ -2,6-Mes ₂)GeBu ^t ₃	2960	673	22
Sn(C ₆ H ₃ -2,6-Trip ₂) ₂ {SnMe ₂ (C ₆ H ₃ -2,6-Trip ₂)}	2856.9	689	9
Sn{CH(SiMe ₃) ₂ } ₂	2328	495	25, 26
SnC(SiMe ₃) ₂ CH ₂ C(SiMe ₃) ₂	2323	484	27
SnC(SiMe ₃) ₂ SiMe ₂ CH ₂ SiMe ₂ C(SiMe ₃) ₂	2299	546	28
Sn(Trip) ₂ C ₆ H ₃ -2,4,6-{CH(SiMe ₃) ₂ } ₃	2208	561	29
Sn(C ₆ H ₃ -2,6-Mes ₂) ₂	1971	553	11
Sn(Bu ^t)C ₆ H ₃ -2,6-Trip ₂	1904	485	24
1	2319	577	this work
2	2116	569	this work
3	2316	559	this work
4	2228	574	this work
5	2444	575	this work
6	2650	570	this work
7	2543	599	this work
Sn(II)C ₆ H ₃ -2,6-Trip ₂	1140	391	30
Sn(C ₆ H ₂ -2,4,6-Bu ^t) ₂	1105	476	21
Sn(II)C ₆ H ₃ -2,6-Trip ₂	793	395	24
Sn{N(SiMe ₃) ₂ } ₂	776	389	31
Sn{C ₆ H ₂ -2,4,6-(CF ₃) ₃ } ₂	723	345	32

NMR shifts cover a very wide range, ca. 700–3000 ppm, and the n–p absorptions also cover most of the visible region (345–689 nm) of the spectrum.³³ Apart from a general expectation of low shielding due to the low coordination number, it is not possible to rationalize the ¹¹⁹Sn NMR chemical shifts on the basis of the σ -electron-donor characteristics of the ligands.⁷ For example, species such as Sn{N(SiMe₃)₂}₂ (δ 776)³¹ or Sn(Cl)C₆H₃-2,6-Trip₂ (δ 793),⁹ which are substituted by one or two electronegative atoms, are observed further upfield than species such as Sn{CH(SiMe₃)₂}₂ (δ 2328)²⁶ or Sn(C₆H₃-2,6-Mes₂)GeBu^t₃ (δ 2960).²² Inductive effects undoubtedly play a role in determining the ¹¹⁹Sn NMR chemical shifts, as do the steric properties of the ligand, which can impose wide interligand angles (and presumably lower singlet–triplet energy separations) at the tin center, but these effects can be swamped by paramagnetic shielding⁷ which is dependent on the energy separation of the singlet ground and triplet excited states.³⁴ Electronegative substituents cause the energy of the tin lone pair to be lower and the singlet–triplet energy difference to increase. This results in a smaller contribution by the paramagnetic shielding term in the tin compounds that have more electronegative ligands. The wavelength at which light is absorbed is related to

(20) Lappert, M. F.; Cardin, D. J.; Keppie, S. A.; Litzow, M. R.; Spalding, T. R. *J. Chem. Soc. A* **1971**, 2262.

(21) Weidenbruch, M.; Schlaefke, A.; Schäfer, A.; Peters, K.; von Schnering, H.-G. *Angew. Chem., Int. Ed. Engl.* **1994**, *33*, 1846.

(22) Setaka, W.; Sakamoto, K.; Kira, M.; Power, P. P. *Organometallics* **2001**, *20*, 4460.

(23) Pu, L.; Power, P. P.; Boltes, I.; Herbst-Irmer, R. *Organometallics* **2000**, *19*, 352.

(24) Eichler, B. E.; Pu, L.; Stender, M.; Power, P. P. *Polyhedron* **2001**, *20*, 551–556.

(25) Davidson, P. J.; Harris, D. H.; Lappert, M. F. *J. Chem. Soc., Dalton Trans.* **1976**, 2268.

(26) Zilm, K. W.; Lawless, G. A.; Merrill, R. M.; Millar, J. M.; Webb, G. G. *J. Am. Chem. Soc.* **1987**, *109*, 7236.

(27) Kira, M.; Yauchibara, R.; Hirano, R.; Kabuto, C.; Sakurai, H. *J. Am. Chem. Soc.* **1991**, *113*, 7185.

(28) Eaborn, C.; Hill, M. S.; Hitchcock, P. B.; Patel, D.; Smith, J. D.; Zhang, S. *Organometallics* **2000**, *19*, 49.

(29) Tokitoh, N.; Saito, M.; Okazaki, R. *J. Am. Chem. Soc.* **1993**, *115*, 2065.

(30) Pu, L.; Olmstead, M. M.; Power, P. P.; Schiemenz, B. *Organometallics* **1998**, *17*, 5602.

(31) Wrackmeyer, B. In *Unkonventionelle Wechselwirkungen in der Chemie Metallischem Elemente*; Krebs, B., Ed.; VCH: Weinheim, Germany, 1992; p 111.

(32) Grützmaker, H.; Pritzkow, H.; Edlmann, F. *Organometallics* **1991**, *10*, 23.

(33) Several other two-coordinate tin(II) molecules with more electronegative ligands have been prepared and structurally characterized. However, complete spectroscopic data are not always available. Examples are Sn(OC₆H₃-2,6-Bu^t)₂^{33a} and Sn{N(SiMe₃)₂}OC₆H₂-2,4,6-Bu^t₃^{33b} (¹¹⁹Sn NMR: δ 277). No UV–vis data are currently available for these, but it can be reasonably expected that the n–p absorptions occur below 400 nm. (a) Barnhart, D. M.; Clark, D. L.; Watkin, J. G. *Acta Crystallogr., Sect. C* **1994**, *50*, 702. (b) Braunschweig, H.; Chorley, R. W.; Hitchcock, P. B.; Lappert, M. F. *J. Chem. Soc., Chem. Commun.* **1992**, 1311.

(34) The reader will be aware that the n–p orbital energy separation is not the same as that of the singlet and triplet states, owing mainly to differing interelectronic repulsion in the ground and excited states.

Table 3. Selected Bond Lengths (Å) for Compounds 1–7

	1 (M = Cr, Ar = Mes)	2 (M = Mo, Ar = Mes)	3 (M = W, Ar = Mes)	4 (M = Cr, Ar = Trip)	5 (M = Mo, Ar = Trip)	6 (M = W, Ar = Trip)	7 (M = Mo, Ar = Trip)
M–Sn	2.816(3)	2.9045(10)	2.9107(10)	2.8474(7)	2.8960(9)	2.9030(8)	2.8941(4)
M–C(Cp)	2.197(19)	2.343(4)	2.332(10)	2.210(4)	2.352(4)	2.185(8)	2.344(4)
	2.197(18)	2.344(5)	2.344(9)	2.221(4)	2.361(4)	2.325(9)	2.345(3)
	2.208(17)	2.348(5)	2.347(10)	2.221(4)	2.361(4)	2.352(10)	2.365(3)
	2.20(2)	2.352(5)	2.353(10)	2.232(4)	2.364(4)	2.363(10)	2.365(3)
	2.140(19)	2.353(4)	2.354(9)	2.221(4)	2.366(4)	2.360(10)	2.394(3)
O–C	1.18(2)	1.152(5)	1.172(11)	1.170(5)	1.155(5)	1.145(15)	1.160(4)
	1.15(2)	1.146(5)	1.188(12)	1.165(5)	1.149(5)	1.147(12)	1.149(4)
	1.15(2)	1.142(5)	1.164(12)	1.165(5)	1.156(6)	1.169(14)	1.154(4)
Sn–C	2.140(19)	2.204(4)	2.200(9)	2.214(4)	2.191(3)	2.185(8)	2.214(3)
M–C(CO)	1.832(18)	1.970(4)	1.942(11)	1.857(4)	1.958(5)	1.951(13)	1.978(4)
	1.84(2)	1.970(5)	1.961(10)	1.850(4)	1.981(5)	1.974(14)	1.978(3)
	1.837(19)	1.980(4)	1.964(10)	1.862(4)	1.967(5)	1.979(12)	1.981(4)
M–Cent(Cp)	1.847	2.019	2.013	1.861	2.027	2.0903	2.030

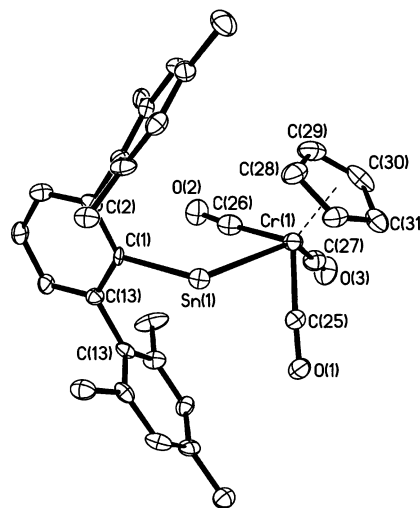
Table 4. Selected Bond Angles (deg) for Compounds 1–7

	1 (M = Cr, Ar = Mes)	2 (M = Mo, Ar = Mes)	3 (M = W, Ar = Mes)	4 (M = Cr, Ar = Trip)	5 (M = Mo, Ar = Trip)	6 (M = W, Ar = Trip)	7 (M = Mo, Ar = Trip)
C(1)–Sn–M	111.0(4)	106.7(10)	110.8(2)	110.12(9)	110.14(10)	109.9(2)	112.10(8)
Sn–M–C(CO)	69.8(6)	69.59(13)	69.0(3)	72.66(12)	72.8(3)	72.8(3)	70.49(10)
	74.2(6)	74.15(12)	74.1(2)	73.84(12)	74.24(13)	74.3(3)	73.16(9)
	133.0(6)	132.63(13)	103.7(4)	136.30(13)	135.1(3)	135.1(3)	133.63(10)
Sn–M–C(centroid)	107.7	106.8	107.0	105.0	103.9	104.2	105.9
Sn–C(1)–C(2)	122.6(12)	120.3(3)	119.7(6)	116.1(3)	117.3(2)	116.9(5)	127.4(2)
Sn–C(1)–C(6)	120.6(12)	119.8(3)	120.5(6)	123.5(3)	122.4(3)	122.9(6)	111.8(2)
C(2)–C(1)–C(6)	121.8(15)	119.8(4)	119.7(8)	120.1(3)	120.1(3)	119.9(7)	119.8(3)
C(1)–C(2)–C(Ar)	115.2(16)	117.1(3)	118.2(8)	117.3(3)	117.6(3)	118.0(7)	121.3(3)
C(1)–C(6)–C(Ar)	115.8(16)	118.1(3)	116.1(8)	117.6(3)	118.0(3)	117.6(7)	117.4(3)
O–C–M	168.8(16)	172.3(4)	172.8(7)	170.0(3)	171.0(4)	172.9(9)	172.7(3)
	175.5(17)	177.2(4)	176.0(8)	174.0(4)	174.5(4)	175.3(9)	175.3(3)
	179.4(19)	178.3(4)	176.9(9)	175.2(4)	176.7(7)	177.4(17)	178.1(3)
C(centroid)–M–C(CO)	118.9	120.5	120.6	118.5	120.4	120.6	120.3
	123.8	126.3	126.4	122.6	124.1	123.9	124.4
	125.3	127.5	127.6	130.7	132.9	133.4	127.6

the singlet–triplet energy difference. Generally speaking, the compounds that appear furthest downfield (least shielded) carry electron-releasing alkyl, silyl, germyl, or stannyl ligands, whereas those that appear furthest upfield have more electronegative substituents. This is opposite to what is expected on the basis of σ inductive effects. For example, the furthest downfield (least shielded) ^{119}Sn NMR shifts in Table 2 are observed for the compounds $\text{Sn}(\text{C}_6\text{H}_3\text{-2,6-Mes}_2)(\text{GeBu}^t_3)$ (δ 2960)²² and $\text{Sn}(\text{C}_6\text{H}_3\text{-2,6-Trip}_2)(\text{SnMe}_2\text{C}_6\text{H}_3\text{-2,6-Trip}_2)$ (δ 2856.9),²⁴ which have absorptions at the longest wavelengths (lowest energies) of 673 and 689 nm, whereas the furthest upfield shifts are observed for $\text{Sn}\{\text{N}(\text{SiMe}_3)_2\}_2$ (δ 776)^{25,31} and $\text{SnCl}(\text{C}_6\text{H}_3\text{-2,6-Trip}_2)$ (δ 793),⁹ which display absorptions at 389 and 395 nm, respectively, in their UV–visible spectra. It should be noted that the correlation between shifts and absorption wavelengths is simplistic and ignores the other factors that influence chemical shift: i.e., σ -donor character of the ligands, steric factors which affect the interligand angle at tin, geometric constraints imposed by the incorporation of tin in a ring structure, possible π -bonding involving the ligands and tin, interelectronic repulsions, weak interactions between tin and other ligand atoms, and hyperconjugative effects. Some of these factors may explain deviations of molecules such as $\text{Sn}(\text{C}_6\text{H}_2\text{-2,4,6-Bu}^t_3)_2$ ²¹ and $\text{Sn}(\text{Bu}^t)\text{C}_6\text{H}_3\text{-2,6-Trip}_2$ ²⁴ from the general trend or variation within the series of compounds 1–7.

Structures. The structures of 1–7 were determined by X-ray crystallography. Crystals of 1–3 are isomorphous, as are those of 4–6. Selected bond distances and

angles are given in Tables 3 and 4, and the structures of 1, 7, and 6 are illustrated in Figures 1–3, respectively. All compounds have very similar structures in which the main features of interest are the transition-metal–tin distances and the interligand angle at tin. The chromium complexes 1 and 4 have Cr–Sn bond lengths of 2.816(3) and 2.8474(7) Å, along with Cr–Sn–C(1) angles of 111.0(4) and 110.12(9)°. The longer Cr–Sn distance in 4 may be due to the more sterically crowded environment caused by Pr^i substitution on the flanking aryl rings. The Cr–Sn distances are ca. 0.1 Å longer than those observed in other Cr/Sn species such

**Figure 1.** Thermal ellipsoid (30%) plot of 1. H atoms are not shown.

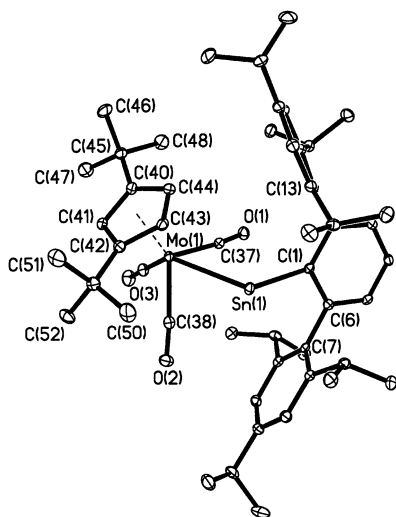


Figure 2. Thermal ellipsoid (30%) plot of **7**. H atoms are not shown.

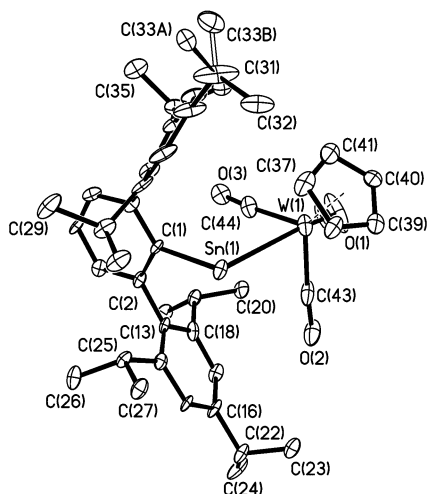


Figure 3. Thermal ellipsoid (30%) plot of **6**. H atoms are not shown.

as $\{(\eta^5\text{-C}_5\text{H}_5)(\text{CO})_3\text{Cr}\}_2\text{SnCl}_2$ ³⁵ (average Cr–Sn = 2.698(4) Å), $(\eta^5\text{-C}_6\text{H}_6\text{D})(\text{CO})_3\text{CrSnPh}_3$ (Cr–Sn = 2.713(1) Å).³⁶ They are also somewhat longer than the sum of the covalent radius of tin (1.4 Å)³⁷ and the metallic radius

of chromium (1.29 Å).³⁸ The Cr–Sn bond lengthening in **1** and **4** may be associated with the steric demands of the terphenyl substituent or the increased p character of the orbital used for Sn–Cr bonding. Furthermore, the effective metallic radii of metals are affected by the ligand set employed. However, the Sn–C bond lengths in all complexes, which are in the range 2.140(19)–2.214(3) Å, are typical for Sn–C compounds and show little evidence of lengthening. The molybdenum and tungsten complexes **2** and **3** and **5**–**7** display M–Sn (M = Mo, W) and Sn–C distances near 2.90 and 2.20 Å. The very small variation in M–Sn bond lengths across these five compounds is consistent with the similar sizes of molybdenum and tungsten.³⁸ The M–Sn bonds are 0.05–0.1 Å longer than the Cr–Sn bonds, and this is consistent with the larger sizes (i.e., 1.40 and 1.41 Å metallic radii for Mo and W)³⁸ of the second- and third-row elements in comparison to those of the first row. However, the M–C distances display a difference of ca. 0.14 Å between the chromium complexes **1** and **4** and the molybdenum and tungsten complexes. Nonetheless, the M–C($\eta^5\text{-C}_5\text{H}_5$) and M–C(CO) bond lengths are very similar to those observed previously in the dimers $[\text{M}(\eta^5\text{-C}_5\text{H}_5)(\text{CO})_3]_2$.^{39,40}

Acknowledgment. We are grateful to the National Science Foundation for financial support.

Supporting Information Available: Tables giving full details of the crystallographic data and data collection parameters, atom coordinates, bond distances, bond angles, anisotropic thermal parameters, and hydrogen coordinates. This material is available free of charge via the Internet at <http://pubs.acs.org>.

OM020583G

(35) Stephens, F. S. *J. Chem. Soc., Dalton Trans.* **1975**, 230.

(36) Djukic, J.-P.; Rose-Munch, F.; Rose, E.; Sims, F.; Dromzee, Y. *Organometallics* **1995**, *14*, 2027.

(37) Wells, A. F. *Structural Inorganic Chemistry*, 5th ed.; Clarendon: Oxford, U.K., 1984; p 1279.

(38) Pauling, L. *The Nature of the Chemical Bond*, 3rd ed.; Cornell University Press: Ithaca, NY, 1960; p 257.

(39) Adams, R. D.; Collins, D. M.; Cotton, F. A. *J. Am. Chem. Soc.* **1974**, *96*, 749.

(40) Adams, R. D.; Collins, D. M.; Cotton, F. A. *Inorg. Chem.* **1974**, *13*, 1086.